Characteristics of an EHD Impinging Dielectric Liquid Jet in Blade-Plane Geometry

Zelu Yan, Christophe Louste,
Philippe Traoré and Hubert Romat
PPRIME Institute,
CNRS-University of Poitiers-ESMA,
Department of Fluid Flow,
Heat Transfer and Combustion,
Bd Marie et Pierre Curie, BP30179,
86962 Futuroscope Chasseneuil Cedex, France
zelu.yan@univ-poitiers.fr

***Abstract* -- An impinging jet in a dielectric liquid is produced by applying a high potential difference to a blade-plane geometry. This kind of jet is both a fluid flow and an electrical phenomenon. In our study, an overview of flow field is easily obtained by using the classical particle velocity method. Two patterns of electrohydrodynamic velocity profiles of jet can be observed when the applied high voltage varies. A typical method for classical impinging jet is used in order to point out the specific characteristics of electrohydrodynamic jets. Electric current measurements are made at the same time of the particle image velocimetry investigations which contributes to the analysis of this electrohydrodynamical phenomenon. Two electrical current regimes are presented according to the potential difference.**

***Index Terms*--Blade-plane geometry, Dielectric liquids, Electric potential, Electrohydrodynamics, Fluid flow control, Particle Image Velocimetry.**

I. NOMENCLATURE

V_x, V_y, V_z, V	The three velocity components in Cartesian Coordinates and their vector norms. For a 2D flow in *xy* plane, $V = \sqrt{{V_x}^2 + {V_y}^2}$.
$\bar{V}_c$	The mean streamwise distribution of centerline velocity.
$\bar{V}_{c\,max}$	The maximum value of $\bar{V}_c$.
$\bar{V}_{1/2}$	The mean velocity corresponding to the position of the half width of jet.
v'_c	The velocity fluctuation in centerline.
x, y, z	The three position components in Cartesian Coordinates.
I_c	The centerline turbulent intensity
H	The blade-plane distance.
$b_{1/2}$	The half width of EHD jet.
I_{total}	The total current in the bulk.
E_m	The mean electric field.

II. INTRODUCTION

An electrohydrodynamic impinging jet in a dielectric liquid can be described as an electroconvective flow induced with the aid of a high potential applied between two electrodes. It is emitted by a sharp electrode and then impinges normally on a second plane electrode. In recent years, this kind of jet widely draws our attention not only for its many industrial applications like heating, cooling and cleaning the electronic components, but also for its interesting geometry, structure and its low power consumptions. When a high enough potential difference is applied between blade-plane electrodes immerged in liquid, a Coulomb force induced by the electric field is exerted on the space charge and then induces the flow motion [1]. In dielectric liquids, space charges (ions) are mainly created by two electric mechanisms: one is the dissociation and recombination phenomenon [2], the other one is the charge injection [3]. It has been demonstrated that in blade plane geometry the dissociation/recombination phenomenon induces a flow from plane to blade [4]-[6] while liquid flows in the opposite direction when an injection occurs [7]. In our experiments, electroconvective flows are directed toward the plane. An injection is generated at the blade tip which has a very small radius of curvature. The injected current is associated with the ion-drag motion of the liquid [8] while the conduction current that occurs on the blade surfaces does not induce any motion. Only a few experimental data can be found in literature about the electroconvective flows induced by charge injection [9]-[11]. In order to complete our knowledge of these jets, a classic Particle Image Velocimetry (PIV) method is used to record the velocity flow field.

PIV method has been recently well adapted to electroconvective flows [12]. It has been successfully used to record an EHD jet flow but in a confined geometry [8]. Unlike study proposed by Daaboul et al., the EHD jet presented in this study is not confined. Then results can be compared to thermal plumes [13] or typical plane jets [14].

From the experimental data, it is possible to analyze the development of the jet under both electrical and mechanical characteristics.

III. EXPERIMENTAL FACILITY

An experimental set up is presented in Fig 1. It consists of a PIV measurement apparatus (2), (4) and the experimental cell (3). Cells (3) is composed of a 30cm x 30cm x30cm plastic tank filled with the dielectric liquid. The electrical device which is a blade-plane geometry, is totally immerged in the liquid. In each wall of the tank, a 18cm x18cm glass window is insert in order to let the laser sheet in. All the other parts of the tank are made of black plastic materials which can absorb laser effectively and avoid the laser reflections. A 10cm long stainless steel blade is installed at the bottom of the lid of the tank. The flat plane electrode is placed perpendicular to the blade. The distance between the blade tip and flat plane can range from 1cm to 4cm which is considered as a main parameter to characterize the jet flow. The negative electrical potential difference (0-40kV) applied between the two electrodes is also another important parameter. The negative voltage is produced by the use of a high voltage power supply Spellman SL1200 in this research. An oscilloscope is used to record the electric current in a closed loop by measuring the voltage shunt of a resistance.

With the aid of a displacement system (1), the CCD camera can be easily operated in two directions. It can record a small scale zone of a 3cm x 3cm square with more detailed information or the large scale of more than 20cm x20cm square region with complete view of the flow field when moved along the *z*-axis.

A rotating tray is installed in the sliding runners. The tank fixed on the tray can rotate and move along *z*-axis which permits either the measurement in the *xy* as well as *yz* plane.

An example of velocity modulus and velocity field is shown in Fig. 2: font view *yz* plan (Fig. 2a) and side view *xy* plan (Fig. 2b). A 90 º rotation of the tank is necessary to obtain these two plans.

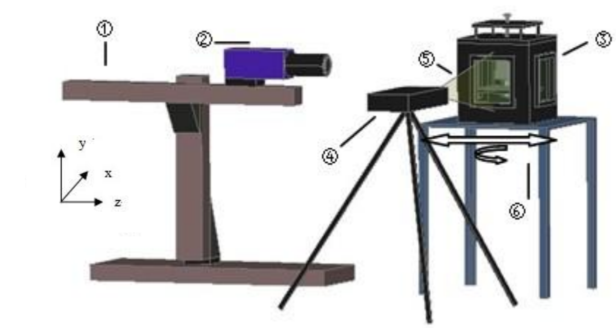

Fig. 1. Experimental facility: (1)-displacement systems; (2)-CCD digital camera; (3)-experimental cell;(4)-double pulse Nd:YAG laser; (5)-laser sheet; (6)-supporter platform

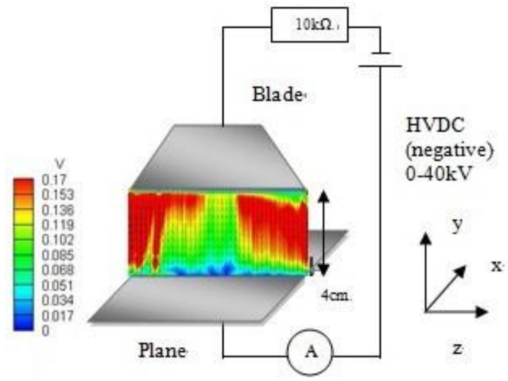

Fig. 2a. *yz* plane for the PIV measurement

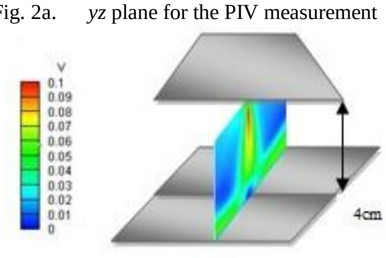

Fig. 2b. *xy* plane for the PIV measurement

The experimental liquid used is an oil with low conductivity. Characteristic of this dielectric oil of 20 ℃ (main experimental temperature) is given in Table I. The increase in temperature caused by the laser heating is very limited that it could be neglected. It has been verified that the time-averaged liquid temperature remains constant. PIV measurements have also proved that local thermal velocity does not exceed a few millimeters per second. One reason is that the laser frequency used is only 4Hz which is too weak to accumulate heat in a short period of time, and another is that the huge bulk liquid is about 18 liters, so the experiment process is considered as an isothermal one.

TABLE I
CHARACTERISTICS OF TEST OIL AT 20 ℃

Parameter	Unit	Value
Density	kg/m^3	850
Kinematic Viscosity	mm^2/s	$4.3.10^{-6}$
Electrical conductivity	S/m	$1.15.10^{-9}$
Relative permittivity		2.2

IV. RESULTS

A. *Two dimensional flow*

A practical ordinary plane jet is produced by a rectangular long narrow slit [14]-[16].

In this study, the EHD jet is generated by a high voltage source applied to a blade electrode, the geometry of the blade is similar to a slot but the ratio of the blade width to its length is almost equal to zero. So the blade-plane device can be considered as 2D geometry.

Fig. 3 presents an *yz* plane PIV measurement when applied a -30kV high voltages with a 3cm blade-plane distance. This PIV velocity field is an overview of the velocity field in the blade front view plane which brings out details in the whole field. The *z* component of the velocity is shown with a background color map, and the mean flow velocity vectors are superimposed on it. The velocity vectors indicate that the main direction of this flow is from blade to the plane (*y*-axis). The green color reveals a low V_z in the middle of the blade, but the red and blue ones show that the liquid flows in the *z* direction at the blade edge vicinity. A symmetrical distribution of the velocity values (V_z) exist between the left and right part.

It is probably due to the generation of a stronger electric field and then a greater charge injection at the two blade edges which repels the liquid from the middle towards the edges.

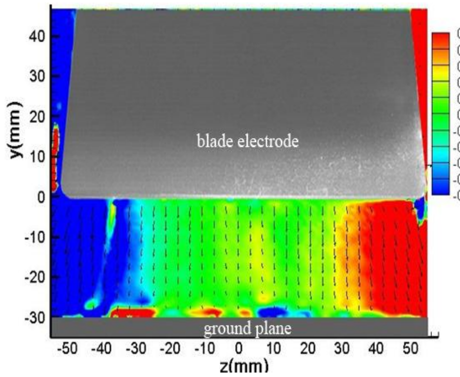

Fig. 3. Color map V_z (m/s) and velocity vectors in the *yz* plane for *x*=0

It is probably impossible to obtain experimentally a pure 2D flow, but in our experiment, the green color in Fig. 3 reveals that in the middle area of the blade, the V_z is smaller than 4mm/s (green color), and the insignificant ratio of V_z/V_y is equal to 0.2%, so it is assumed that the flow can be considered as 2D in the middle of the blade. In this study, investigations in *xy* plan are conducted at *z*=0 position to ensure the two dimensional flow.

B. Electric field depending EHD jet

Fig. 4 shows the time-averaged velocity field calculated by 1000 instantaneous measurements. In fact, convergence of local time-averaged velocity has been reached after 700 frames calculations.

For a given distance, two different patterns of jet which depend on the applied potential have been observed, Fig. 4 show the case for a 4cm blade plane distance.

Fig. 4a represents one pattern of EHD flow. When the potential difference is less than 5kV, a non symmetrical and unstable jet is produced. It starts at the blade tip and dissipates in the bulk after a short downstream distance. It seems that except in the near field region, the viscosity force dominates over the electrical force which prevents the jet from reaching the plane electrode. A statistical analysis of instantaneous velocity has demonstrated that a highly intermittent behavior is observed. Sometimes the jet flow can even be turned off. These fluctuations might be due to a weak electrical field, and the electric field at the blade tip is probably close to the threshold value of injection.

This dissipated-like jet has the similar characteristics with classical jets at low Reynolds number investigated by Abdel [15].

Fig. 4b represents a typical jet which can be obtained with a potential varying from 5kV to 15kV, a more stable jet with a greater velocity is generated. Because of the wider range of jet, more liquid is drawn towards the blade electrode in the near field due to the entrainment effect. With the two wall jets formed along the plane surface, two large counter-rotating turbulent vortices have been induced on either part of the jet.

Fig. 4c is obtained when the potential is greater than 15kV, this jet shape can be compared to a classical impinging jet. Both main jet and wall jets become thinner, and the velocity increases with voltage. Note that the potential difference is not a fix parameter to distinguish this two pattern jet. For 1cm, the pattern (Fig. 4c) is reached when a -10kV potential is applied to the blade, so mean electric field defined by ratio of applied voltage and electrode gap distance is a more appropriate reference.

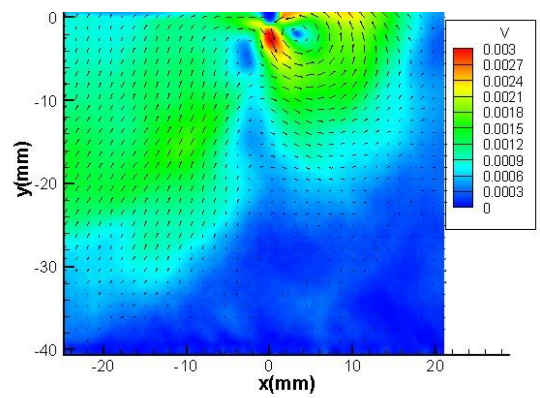

Fig. 4a. Color map of velocity modulus (m/s) and velocity vectors in the *xy* plane for a 5kV EHD jet, *H*=4cm

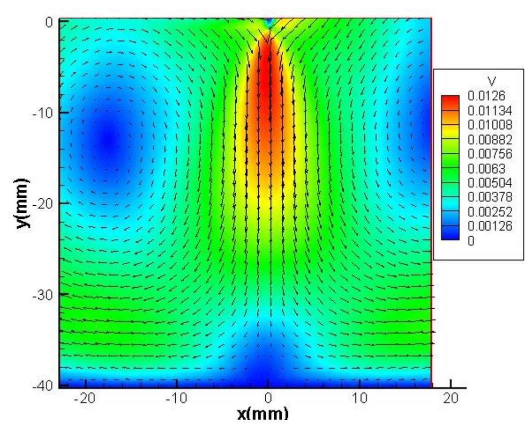

Fig. 4b. Color map of velocity modulus (m/s) and velocity vectors in the *xy* plane for a 10kV EHD jet , *H*=4cm

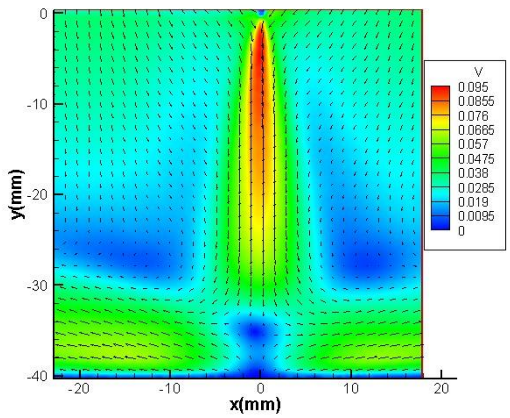

Fig. 4c. Color map of velocity modulus (m/s) and velocity vectors in the *xy* plane for a 40kV EHD jet, *H*=4cm

C. Axial velocity of EHD jet

Fig. 5 shows the dimensionless centerline velocity (along *y*-axis) evolution with the dimensionless blade-plane gap (*H*=4cm). The velocity is non-dimensionalized by the maximum centerline velocity $\bar{V}_{c\,max}$, and the characteristic distance is the electrode gap *H*. Note that the jet obtained with a 5kV voltage and a 4cm gap is instable. Under such conditions, it is hard to reach a convergence value within the range of 1000 frames measurements. So only axial velocity profiles for different applied voltages ranging from -10kV to -40kV have been plotted in Fig. 5.

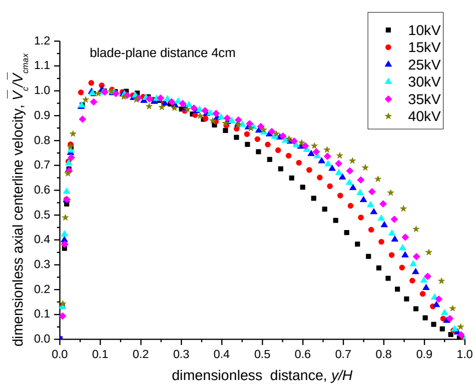

Fig. 5. Centerline velocity evolution of the EHD jet for various applied potentials with 4cm blade-plane distance

The centerline velocity curves are plotted from the blade tip *y/H*=0 to the plane electrode *y/H*=1 (Fig. 5). For each curve, the velocity firstly increases quickly and reaches a maximum value. Downstream from this acceleration zone, a pseudo-developed zone is visible. In this zone all curves are superimposed .The last zone is a deceleration zone caused by impinging on the plane. The length of the acceleration zone is the distance of the jet centerline between the electrode tip and the maximum velocity point. It is noted that this zone length is nearly constant and is located at *y/H*=0.1 for all voltages. This behavior can probably be interpreted by the space charge distribution around the blade tip vicinity. It could be a consequence of space-charge-limited current. If the evolution of electric field in the centerline follows the same mathematical laws for all the voltages, it explains why the maximum velocity position in the centerline remains constant. Then the voltage can only change the absolute dimensional value, but not the evolution laws.

The viscosity force influence is very limited compared to the electrical force at the near field, the acceleration rate of the centerline velocity slowly decreases which partly correspond to the decay of the electrical field (force) in the centerline, and the maximum point of velocity means that the balance between electrical and mechanical forces has been reached.

At the beginning of the pseudo-developed zone, the centerline velocity curves are overlapping and show a quasi-linear decrease for all applied voltages until certain distance. This distance depends on the voltage and then begins to decline sharply. For the -10kV case, the jet enters into the impinging zone at *y/H*=0.3, while for the -40kV case, it occurs at *y/H*=0.8. Such quite linear overlapping behavior can also be observed in classical jets. It is called self-similar region. It corresponds to a region of fully developed turbulent. But this behavior is observed far from the injector in classical jet. It means that EHD jets are highly turbulent. The charge injection in low viscosity liquids is not a smooth phenomenon but mainly composed of many violent pulses of electric charges which induce turbulence.

D. Lateral profiles of velocity

Fig. 6 reports the dimensionless lateral distribution of velocity profiles ($\bar{V}/\bar{V}_c$) at *y/H*=0.5 location. On the *x*-axis, distance is normalized by using the velocity half-width $b_{1/2}$, which is defined as the lateral location where the velocity meets the condition: $\bar{V}_{1/2}=0.5\bar{V}_c$, as reported in [17]. The lateral velocity profiles give a self-similar distribution with increased voltage. This behavior is also observed in classical impinging jets.

The Gaussian fit (green line) agree well with the velocity distribution for a higher potential when taking account into an initial offset value which is caused by the global flow motion of the liquid in the tank.

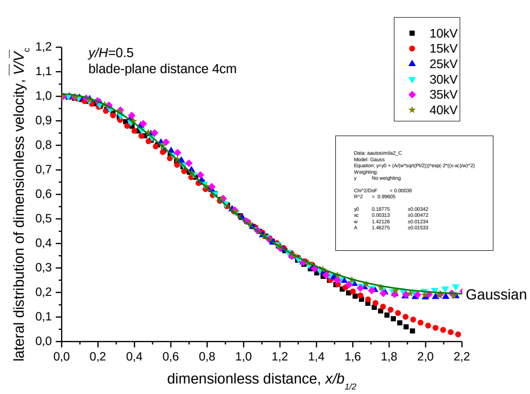

Fig. 6. Non-dimensionalized velocity profiles distribution of $\bar{V}/\bar{V}_c$ for various applied voltages at position *y/H*=0.5 with 4cm gap

E. *Turbulent intensity of EHD jet*

Fig.7 indicates the centerline evolution of the turbulent intensity versus non-dimensionalized distance from the blade tip. The turbulent intensity *I*, also often referred to as turbulent level, is defined as:

$$I \equiv v'/\bar{V} \quad (1)$$

Where v' is the velocity fluctuation which is equal to its root mean square value and calculated by (2) and (3). Note that for the i^{th} PIV velocity field measurement, we have:

$$v_i' = V_i - \bar{V} \quad (2)$$

$$v' = \sqrt{\sum_{i=1}^{n}(V_i - \bar{V})^2 / \mathrm{n}} = v_{rms} \quad (3)$$

So in the centerline we have the turbulent intensity:

$$I_c \equiv v_c'/\bar{V}_c \quad (4)$$

It can be observed that turbulent intensity decreases gradually from the blade tip of more than 100% to one asymptotic value in the downstream field and then increases again when the flow is near the plane area. The exact level of turbulent intensity in this region is difficult to estimate because in the near field region the electric field is so strong that particles could be charged [12]. Despite this, it is clear that the turbulent intensity is very high at the jet origin. The high level of turbulent intensity which occurs is unusual in classical plane jets. It can be considered as an EHD jet characteristic. It is known that in the near field, an intense electric field is presented and the ions are entrained by the liquid flow which takes the shape of a narrow plume around the axis of centerline [1].

In classical plane jet, turbulent intensity reaches a constant value in the self-similar region. This value is independent of the way for the production of the flow jet and approximately equal to 0.25.

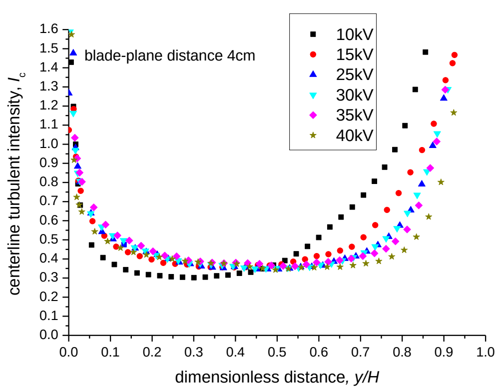

Fig. 7. Streamwise evolutions of turbulent intensity for different potential with 4cm blade-plane distance

In EHD jet, a constant turbulent intensity value is obtained in the middle field of the jet. It presents a voltage independent feature but the value of turbulent intensity is about 0.35. As this area is correspondent to the pseudo-developed zone at which the electrical force has very few influence and the jet flow approaches an asymptotic fully developed state. It will be verified that this turbulence value remains constant for various electrode gap. When a plane gets involved, the jet flow's turbulent intensity increases intensely while its velocity decreases sharply.

F. *Total current in dielectric liquids*

Fig. 8 presents the evolution of total current with mean electric field for different distances. It shows that each current curve is the sum of two parts, the first is a linear one named weak injection regime and the second is a quadratic increase which represents the strong injection or space-charge-limited injection regime [12].

In our study, the injection current is not very clearly exposed because the total current is the sum of the conduction current and the injection one. The important conduction current is due to the large surface of blade electrode.

The growth rate of the total current gradually increases with the increase of electrode gap distance, and an asymptotic value is reached at 4cm distance. This means that beyond this value, and for a voltage below 40kV, the system acts as if the boundary condition was a zero potential at infinity. The jet characteristics are then independent of the electrode gap.

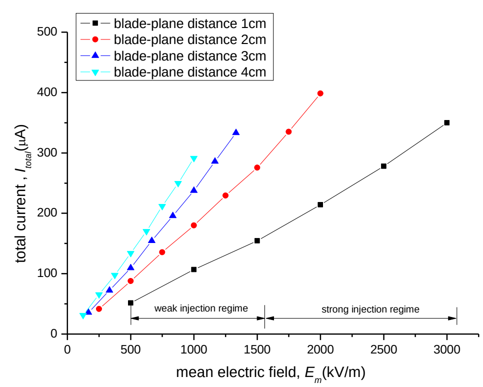

Fig. 8. Evolution of the total current versus mean electric field for different distance.

V. CONCLUSION

Both geometric and electrical parameters have been analyzed for this EHD impinging jet immerged in dielectric liquids.

From PIV measurements of the velocity field between the blade and plane, the jet is assumed to be 2D in a central region. Thus the investigation zone has been fixed in the middle of the blade to ensure a 2D EHD jet. Then time-averaged velocity fields can be classified into two patterns according to pattern jet.

EHD jets have been studied by using the centerline velocity profiles. In comparison with a classic plane impinging jet, the EHD jet reveals a lot of common points. Some specific characteristics have also been underlined.

In the acceleration zone, the acceleration length is independent of the applied voltage. An intense decay is observed in turbulent intensity evolution profiles along the flow downstream direction.

In the pseudo-developed zone, the non-dimensionalized centerline velocity curves overlap for all voltages. Meanwhile the non-dimensionalized of velocity in lateral direction fits well with a Gaussian curve. In this area, the turbulent intensity is constant as in classical plane jet but the value is different.

In the impinging region, the centerline velocity shows a faster decay than that in the pseudo developed zone, and a huge growth of turbulent intensity can be seen.

The current-electric field curve reveals the existence of the process of conduction and injection which are considered as two mechanisms corresponding with the EHD jet.

The current versus electric field curves indicates the presence of two injection regimes: a weak injection regime and a strong one, but it seems that the change of injection mode has a very small influence on the flow field characteristics.

REFERENCES

Periodicals:

[1] A. Castellanos “electrohydrodynamics,” *ISBN 3-211-83137-1, Springer-Verlag*, 1998.

[2] Y. Feng and J. Seyed-Yagoobi, “Understanding of electrohydrodynamic conduction pumping phenomenon,” *Physics of Fluids*, vol. 16, No.7, pp. 2432-2441, 2002.

[3] P. Atten, “Electrohydrodynamic Instability and Motion Induced by Injected Space Charge in Insulating Liquids,” *IEEE Transactions on Dielectrics and Electrical Insulation*, vol. 3, No. 1, pp. 1-17, 1996.

[4] P. Atten and J. Seyed-Yagoobi, “Electrohydrodynamically induced dielectric liquid flow through pure conduction in point/plane geometry,” *IEEE Trans. Dielectr. Electr. Insul*, vol. 10, No. 1, pp. 17-36, 2003.

[5] S. I. Jeong and J. Seyed-Yagoobi, “Experimental study of electrohydrodynamic pumping through conduction phenomenon,” *J. Electrostatics*, vol. 56, pp. 123-133, 2002.

[6] R. Hanaoka, S. Takata, M. Murakumo, and H. Anzai, “Properties of liquid jet induced by electrohydrodynamic pumping in dielectricliquids,” *Electr. Eng. Japan*, vol. 138, Issue 4, pp.1-9, 2002.

[7] P. Atten , B.Malraison and M.Zahn, “Electrohydrodynamic Plumes in Point-plan Geometry,” *IEEE Trans. Dielectr. Electr. Insul*, vol.4, pp. 710, 1997.

[8] M. Daaboul, C. Louste, and H. Romat, “Electrohydrodynamical characteristics of a dielectric liquid flow induced by charge injection,” *J. Electrostatics*, vol. 63, pp. 861-869, 2005. IEEE/ICDL (2008), pp. 66-69, Poitiers, France.

[9] P. Atten and B. Malraison, “Panaches chargés résultant de l'injection d'ions dans un liquide isolant par une lame ou une pointe placée en face d'un plan,” *J. Phys. III France* 4, pp75-85, 1994.

[10] M.Haidara and P. Atten, “Role of EHD Motion in the Electrical Conduction of Liquids in a Blade-Plane Geometry,” *IEEE Transactions on Industry Applications*, vol IA-21, No.4, jun.1995.

[11] Mc Cluskey, F M J and Perez P A, “The electrohydrodynamic plume between a line source of ions and a flat plane,” *IEEE Transactions on Electrical Insulation* ,vol.27, pp. 334–341,1992.

[12] M. Daaboul, C. Louste, and H. Romat, “PIV measurements on charged plumes–Influence of SiO2 seeding particles on the electrical behavior,” *IEEE Trans. Dielectr. Electr. Insu.*,vol. 16 , Issue. 2, pp.335-342, 2009.

[13] Vazquez, P.A.Perez and A.T.Castellanos, “Thermal and electrohydrodynamiqc plumes. A comparative study,” *phys. Fluids*, vol .8 , pp. 2091-2095,1999.

[14] Ravinesh C.Deo, Jianchun Mi and Graham J.Nathan, “The influence of Reynolds number on a plane jet,” *Phys. Fluids*, 20,075108(2008).

[15] A.A.Abdel-Rahman, S.F.AI-Fahed and W.Chakroun, “The near-field characteristics of circular jets at low Reynolds numbers,”*Mechanics Research Communications*, vol.23(3), pp.313-324,1996.

[16] Deo, Ravinesh C, Mi Jianchun, Nathan and Graham J, “The influence of nozzle-exit geometric profile on statistical properties of a turbulent plane jet,” *Experimental Thermal and Fluid Science*, vol.32, pp.545-559, 2007.

[17] Gutmark, E., Wygnanski I., “The planar turbulent jet,” *J. Fluid Mech*, vol. 73, Part 3, pp. 465-495, 1976.